Recent Results in Model-Based Wind Retrieval

D. G. Long *J. Gunther*

Electrical and Computer Engineering Dept., 459 Clyde Build., Brigham Young University, Provo, UT 84602

Abstract - **From multiple measurements of the normalized radar backscatter (σ^o) made by a spaceborne scatterometer, the near-surface wind over the ocean can be inferred using a geophysical model function relating σ^o and the vector wind. Recently, a model-based retrieval technique has been developed. The technique avoids many of the problems associated with traditional point-wise wind retrieval and ambiguity removal. The model-based retrieval can also produce vorticity and divergence fields as auxliary products. In this paper the method is applied to ERS-1 scatterometer data. Comparisons in performance between the traditional two-step point-wise wind retrieval/ambiguity removal method and the model-based retrieval method are presented using simulated and actual ERS-1 measurements. The results suggest that model-based retrieval can produce more accurate estimates of the wind field than point-wise wind retrieval–particularily in low wind speed regions where the C-band model function results in low wind accuracy for traditional wind estimation. We consider the spectra of the wind and wind vorticity over scales of from 50 to 1000 km.**

I. INTRODUCTION

Spaceborne scatterometers are the only proven method for global all-weather measurement of vector winds at the ocean's surface. Such measurements are critical inputs in studies of oceanic circulation and air/sea interaction. The scatterometer does not directly measure the wind. Instead, it measures the normalized radar backscatter (σ^o) of the ocean's surface which is related to the wind via a geophysical model function. From multiple measurements of σ^o the near-surface wind can be estimated using a retrieval (estimation) algorithm. Traditionally, a point-wise approach, in which only the σ^o measurements corresponding to a particular sample point are used to estimate the wind at that sample point, has been used to retrieve winds from the scatterometer measurements. Since point-wise wind retrieval produces non-unique estimates of the wind vector, "dealiasing" or "ambiguity removal" must be used to select a unique wind vector estimate. Algorithms for ambiguity removal remain error-prone.

Recently, a model-based approach to estimating wind fields over the ocean's surface from wind scatterometer measurements has been developed which avoids some of the problems associated with traditional point-wise wind retrieval and ambiguity removal [3,4,5]. In model-based wind retrieval, a model for mesoscale the near-surface wind field is used. The model is based on the geostrophic approximation and simplistic assumptions about the wind field vorticity and divergence, but includes ageostrophic winds. The model parameters are estimated from the scatterometer measurements of the radar backscatter of the ocean's surface using maximum-likelihood (ML) principles: the model parameter vector which maximizes the log-likelihood function is the ML estimate of the model parameters. The wind field estimate is then computed from the estimated model parameters.

In this paper we report preliminary results of the method applied to ERS-1 AMI scatterometer measurements. Comparisons in performance between the traditional two-step wind retrieval/ambiguity removal method and model-based method are presented using simulated radar backscatter measurements. The results suggest that the model-based method can produce more accurate estimates of the wind field than the traditional procedure–particularily in low wind speed regions where the accuracy is low for traditional wind estimation. These results demonstrate the feasibility of the technique for ERS-1 wind retrieval.

Model-based wind retrieval also produces estimates of the wind field vorticity and divergence as auxilary products. We compare the observed vorticity and divergence spectra of winds estimated using SASS and ERS-1 winds. We first describe the model-based estimation procedure, present simulation and actual data results, and then consider spectra of the wind field components and spectra of the voriticty and divergence fields.

II. MODEL-BASED ESTIMATION

The method was originally developed and tested using simulated measurements from the NASA scatterometer (NSCAT) [3,4] and has been successfully applied to Seasat scatterometer (SASS) measurements [5]. Two primary differences between ERS-1 and SASS affecting the application of the model-based wind retrieval method to ERS-1 are 1) the number of azimuthal observations of σ^o and 2) the spatial sampling grid. In the former, ERS-1 has three azimuthal angles whereas SASS had only two. The additional azimuth angle for ERS-1 results in improved "skill" for ambiguity removal for point-wise wind estimation. For model-based estimation, the additional azimuth angle reduces the number of local minimums in the model-based estimation objective function, simplifying the objective function optimization. While the ERS-1 sampling grid is a uniformly spaced 25 km grid with 50-70 km σ^o measurement resolution, the SASS measurements were 50 km resolution cells on an irregular sampling grid. SASS also had a 500-700 kmwide observation swath on both sides of the nadir track while ERS-1 has

This work was supported under contract with the Jet Propulsion Laboratory, California Institute of Technology.

0-7803-1385-2/93/$3.00

only a single 500 km wide swath on one side and, hence, less global coverage. These differences require modification of the implementation of the model-based estimation procedure for ERS-1.

To apply the model-based retrieval procedure, the ERS-1 observation swath is segmented into 500×500 km overlapping regions. Approximately 50% region overlap is provided in both the along- and cross-track directions. The parameters of the wind field model are estimated separately for each region and the resulting wind field estimates averaged to obtain the wind field estimate over the swath.

Model-based retrieval, in effect, assimulates the σ^o measurements directly into a model for the near-surface wind field. To do this, an objective function (the negative log-likelihood function) is formulated for the wind field model parameters. The model parameters which minimize the objective function are the maximum-likelihood (ML) estimate of model parameters. The wind field is then computed from the estimated model parameters. This results in a ML estimate of the wind field. The wind field model is based on the geostrophic approximation and simplistic assumptions about the wind field vorticity and divergence, but includes ageostrophic winds [3]. To simplify computation, a gradient-based optimzation algorithm is used for the minimization of the objective function from an initial value determined from a point-wise wind estimate (see [5]). For this paper a 2nd order parameterized boundary condition (PBC) model is used [3,5].

To evaluate the performance of model-based wind estimation for ERS-1, both simulated and actual ERS-1 measurements have been used. The advantage of the simulation is that the actual true wind field is known, permitting detailed performance evaluation. Preliminary results for simulated measurements are considered below.

III. PERFORMANCE ANALYSIS

To initially evaluate the estimation accuracy, we have adopted a simulation-based approach in which the true wind field is known. We can then compare the true wind with the scatterometer-derived wind. We have used the same simulated wind fields which were used to evaluate and optimize pointwise retrieval for the NASA Scatterometer (NSCAT) [6]. To generate the simulated σ^o measurements, several randomly selected ERS-1 orbits (revs) passing over the Pacific were used as templates. The actual σ^o measurements in these passes were replaced by simulated σ^o measurements computed using the simulated wind field, the geophysical model function, and the actual ERS-1 measurement geometry. Monte Carlo noise was added to the simulated measurements. The geophysical model function used was the Frelich/Dunbar C-band model function [2]. Each true wind field was observed with several orbit templates.

Pointwise ML estimation (traditional wind retrieval) of winds from the simulated σ^o measurements was then done. The ambiguity closest to the true wind was selected as the unique wind vector estimate; thus, the pointwise wind vector estimate represents ideal ambiguity removal, i.e., the best that can be done with pointwise retrieval. For comparison, winds were are also estimated using the model-based approach. Since our initial goal was to demonstrate feasibility, the closest ambiguity field was used to compute the initial value for the optimization to reduce the computational load.

Table 1
RMS estimate errors from simulation.

	Wind Speed Range (m/s)				
	2-4	4-8	8-12	12-20	20+
RMS Speed (m/s)					
Model-based	0.88	1.03	1.19	1.66	2.49
Point-wise*	0.80	0.90	1.17	1.87	2.54
RMS Dir (deg)					
Model-based	16.9	9.3	6.8	5.3	4.5
Point-wise*	39.9	24.6	17.5	14.7	14.9
Vector (m/s)					
Model-based	1.14	1.33	1.60	2.12	2.97
Point-wise*	2.06	2.50	3.08	4.28	5.92

* Ambiguity closest to the true wind.

An illustration comparing point-wise and model-based wind field estimation is shown in Fig. 1. In these figures, winds are plotted on a cross-track/along-track grid. The true simulated wind field sampled at the 25 km grid centers is shown in Fig. 1a. The model-based estimate obtained from the simulated σ^o measurements is shown in Fig. 1b. The closest alias from the point-wise ambiguity set is shown in Fig. 1c, thus Fig. 1c represents the ideal dealiased wind field since an actual dealiased wind field will contain ambiguity selection errors.

Table 1 summarizes the results of our simulation experiment. The total root-mean-square (RMS) errors for each wind retrieval method are presented. The vector error in Table 1 is the RMS of the vector-magnitude of the difference between the true wind vector and the estimated wind vector. Comparison of the model-based and point-wise wind field estimates using simulated data suggest that the model-based wind field estimates: (1) are less "noisy", (2) exhibit smaller RMS vector and direction error than the closest ambiguity field (and therefore, from the result of *any* dealiasing algorithm).

When using actual ERS-1 measurements, the performance of the model-based estimate is difficult to independently establish since the ground truth wind field is not known. However, comparison with the JPL-produced value-added product [Freilich, personal communication] shows the data sets compare very favorably.

IV. SPECTRAL STUDIES

As an approach to validation of model-based retrieval with actual data we consider a spectra-based analysis approach. We consider both the wind component spectra and the spectra of the wind vorticity. To compute the wind component spectra, the one-dimensional (in the along-track direction) wavenumber spectra of the u and v components of retrieved wind fields were computed using an approach similar to Freilich and Chelton [1] but at 50 km resolution. The one-dimensional spectra were separately computed in 4 regions defined by the latitude bands given in Table 2. Within a given latitude band, an along-track sequence of u and v components of the wind was extracted for each cross-track bin. Sequences with gaps or containing land were discarded. The spectral estimates were averaged over multiple orbits to provide an

Table II
Region definitions.

Region	Latitude Range	Longitude Range
1	−45° to −25° N	160° to 280° E
2	−25° to −5° N	160° to 280° E
3	+5° to +25° N	140° to 250° E
4	+25° to +45° N	150° to 230° E

"expected" scatterometer measurement capability. Figure 2 provides plots of the u component spectra estimated from one day of ERS-1 data for each region. For comparison, Fig. 3 provides similar plots from 9 days of SASS data. We note that the spectral rolloff exhibit a power-law dependence on wavenumber $k = 2\pi/\lambda$ of $\sim k^{-2}$ which is consistent with Freilich and Chelton [1].

The resolution and coverage of scatterometer wind measurements are unparalleled for studying atmospheric variability. Of particular interest is the curl of the wind stress which drives ocean circulation. Using a bulk parameterization, the wind stress curl can be related to the vorticity of the near-surface wind. Using model-based retrieval for which the vorticity and divergence fields are auxilary products, SASS and ERS-1 data can provide direct measurements of the wind vorticity (and divergence) at scales from 50 km to over 1000 km; the noise enhancement associated with differencing schemes is eliminated and there are fewer holes in estimated fields. Fig. 1.d illustrates the wind vorticity associated with the model-based estimate shown in Fig. 1.b.

The wind field vorticity and divergence were extracted along the scatterometer cell tracks in 4 latitude bands (see Table 2) over the Pacific Ocean and the average spectra for each latitude region was computed. Figure 4 provides plots of the vorticity spectra estimated from one day of ERS-1 data for each region. For comparison, Fig. 5 provides similar plots from 9 days of SASS data. Both the ERS-1 and SASS vorticity spectra exhibit an average power-law dependence on wavenumber of $\sim k^{-2}$. The difference in rolloff at large wavenumbers (corresponding to small spatial scales) may be due, in part, to the reduced resolution of ERS-1 relative to SASS and the spatial filter applied to the ERS-1 data in computing σ^o from the raw radar measurements. No spatial filter was used on the SASS data.

V. CONCLUSION

We have demonstrated that model-based wind retrieval can be successfully applied to ERS-1 data and that it can be used for studies of the spectra of the wind field and of the vorticity and divergence fields. We note that because the model-based estimation approach takes advantage of the inherent correlation in the wind field over the measurement swath, it is more tolerant of noise in the σ^o measurements than is the point-wise wind estimate technique; the accuracy of the wind fields estimated using a model-based approach degrade gracefully as the SNR of the measurements is reduced. This may permit reductions in the size and weight of future scatterometer instruments by reducing the requirements on the SNR of the σ^o measurements, permitting smaller transmitters, antennas, etc.

VI. REFERENCES

[1] M. H. Freilich and D. B. Chelton, "Wavenumber Spectra of Pacific Winds Measured by the Seasat Scatterometer," *J. Phys. Oceanography*, Vol. 16, No. 4, pp. 741-757, April 1986.

[2] M. H. Freilich and R. S. Dunbar, "A Preliminary C-band Scatteromer Model Functionfor the ERS-1 AMI Instrument," *Proceedings of the First ERS-1 Symposium – Space at the Service of our Environment*, Cannes, France, 4-6 Nov. 1992 ESA SP-359 (March 1993), pp. 79-83.

[3] D. G. Long and J. M. Mendel, "Model-Based Estimation of Wind Fields Over the Ocean from Wind Scatterometer Measurements I: Development of the Wind Field Model", *IEEE Trans. Geosci. Remote Sensing*, Vol. 28. No. 2, pp. 349-360, May 1990.

[4] D. G. Long and J. M. Mendel, "Model-Based Estimation of Wind Fields Over the Ocean from Wind Scatterometer Measurements II: Model Parameter Estimation," *IEEE Trans. Geosci. Remote Sensing*, Vol. 28. No. 4, pp. 361-373, May 1990.

[5] D. G. Long "Wind Field Model-Based Estimation of Seasat Scatterometer Winds," to appear *JGR*, 1993.

[6] S. J. Shaffer, R. S. Dunbar, S. V. Hsiao, and D. G. Long, "A Median-Filter-Based Ambiguity Removal Algorithm for NSCAT," *IEEE Trans. Geosci. Remote Sensing*, Vol. 29, No. 1, pp. 167-174, Jan. 1991.

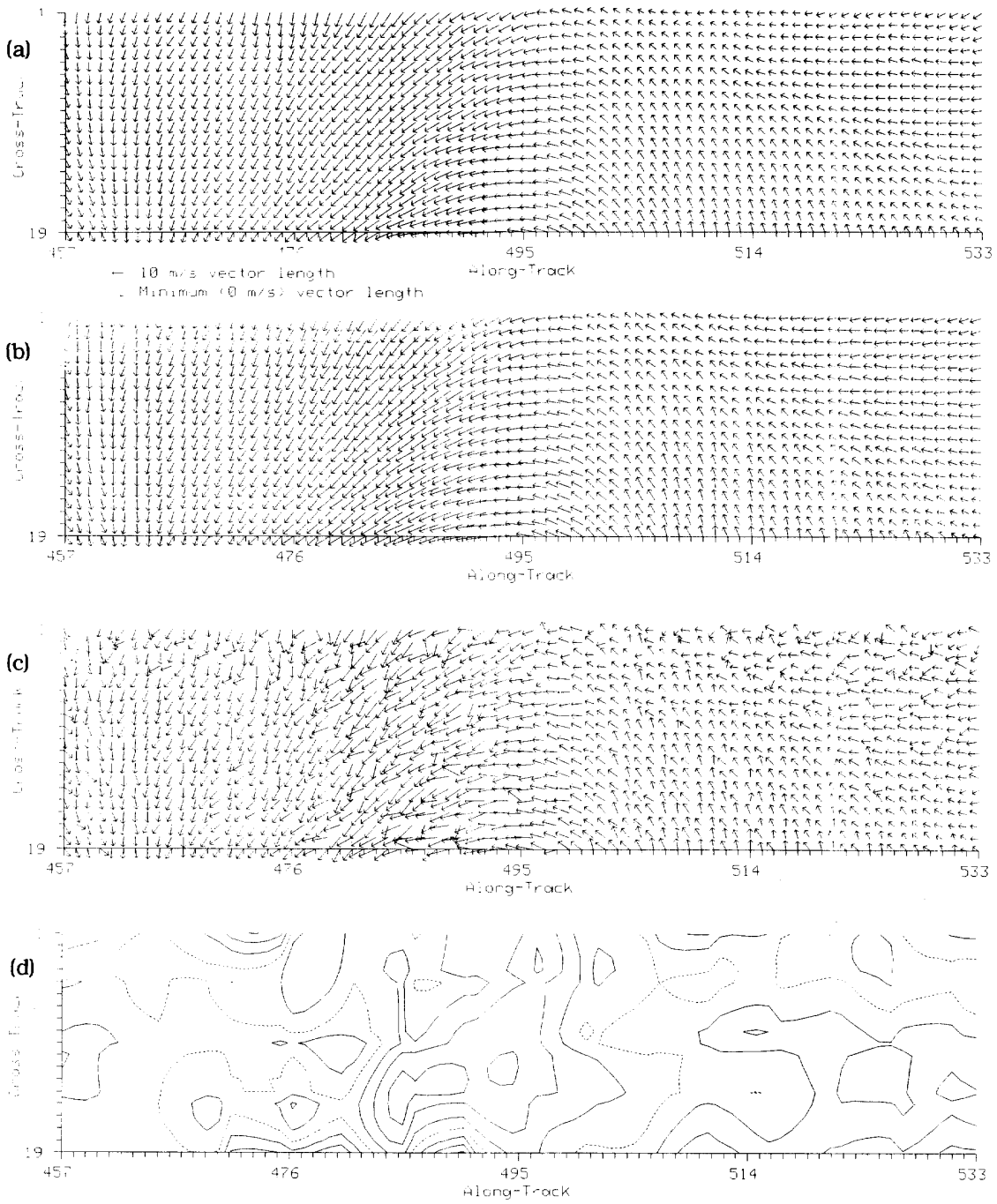

Figure 1. Comparison of wind estimates. (a) True wind field example. (b) Model-based estimate from simulated σ^o measurements. (c) "ideal" dealiased point-wise wind field estimate generated from the same simulated σ^o measurements as (b). The point-wise ambiguity closest to the true wind vector is shown. (d) Wind vorticity estimate generated as an auxilary product of model-based retrieval. The contour levels are arbitrary.

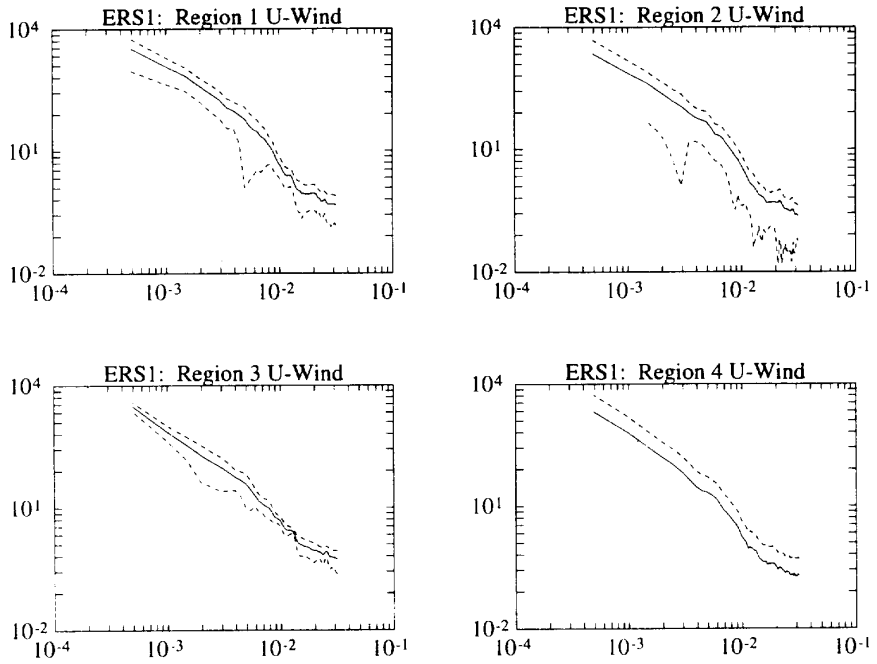

Figure 2. Plots comparing the along-track spectra of the u components of the wind estimates for ERS-1 [illegible] and other spectral plots, the vertical scale is arbitrary. The dashed line indicates the 1-σ confidence interval

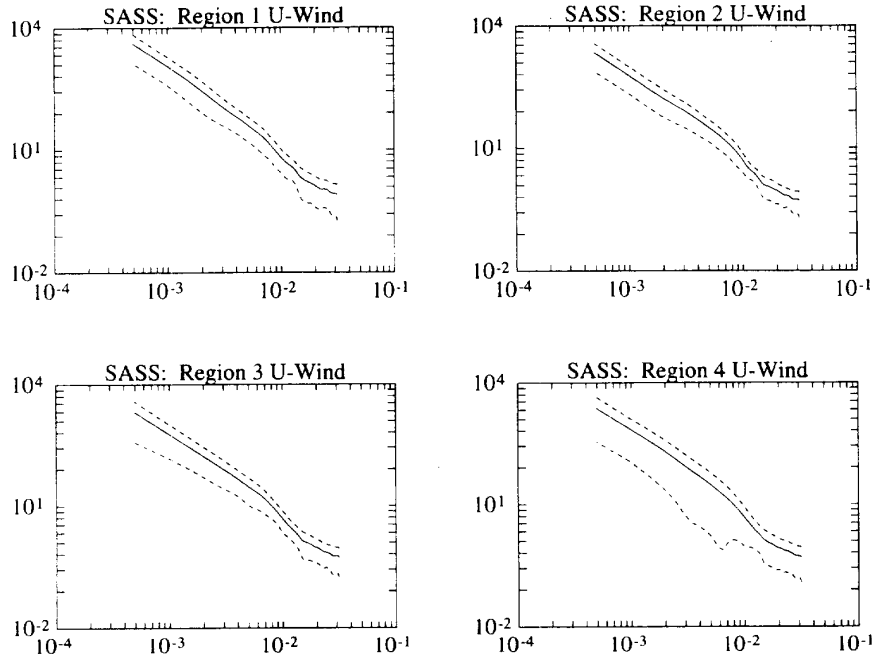

Figure 3. Plots comparing the along-track spectra of the u components of the wind estimates for SASS.

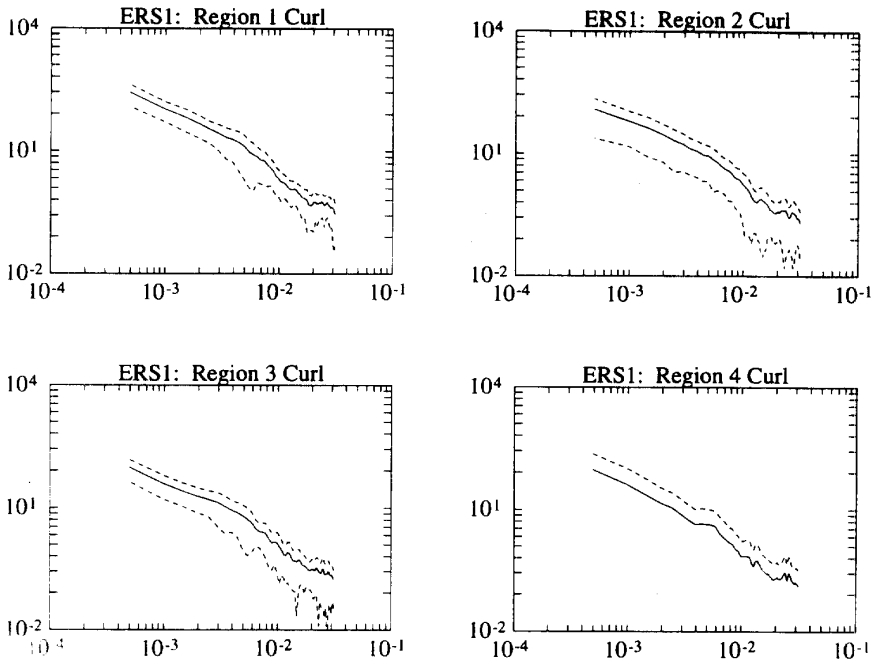

Figure 4. Plots of the observed along-track spectra of the vorticity for ERS-1.

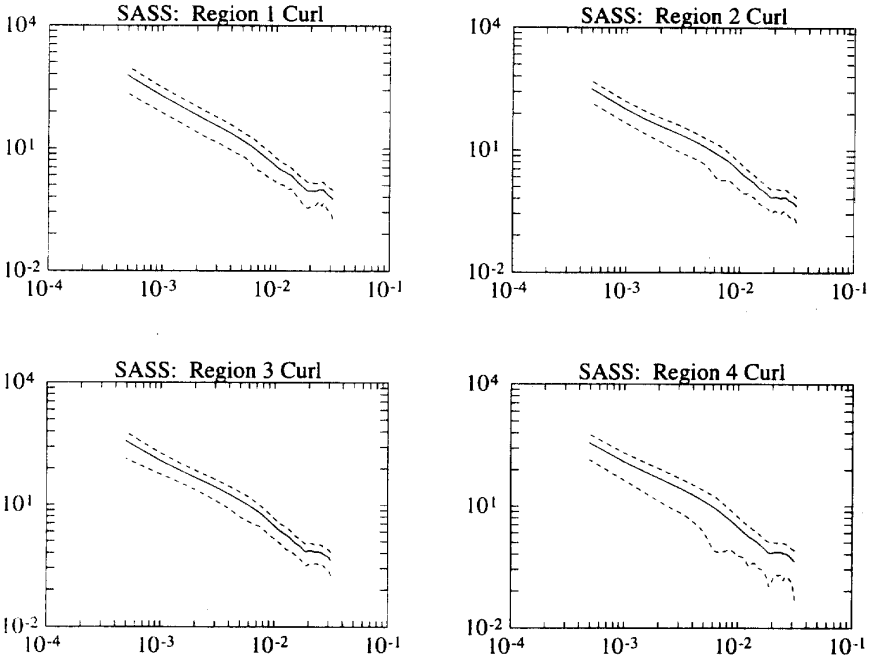

Figure 5. Plots of the observed along-track spectra of the vorticity for SASS.